Magnetoelectric control of surface anisotropy and nucleation modes in L10-CoPt thin-films

Priyanka Manchanda,[1] Pankaj Kumar,[2] Hans Fangohr,[3] David J. Sellmyer,[1] Arti Kashyap,[2] and Ralph Skomski[1]

[1]*Department of Physics and Astronomy and Nebraska Center of Materials and Nanoscience, University of Nebraska, Lincoln, NE 68588, United States*
[2]*School of Basic Sciences, Indian Institute of Technology Mandi, Mandi, HP 175001, India*
[3]*Engineering and the Environment, University of Southampton, Southampton SO17 1BJ, United Kingdom*

Abstract— The interplay between electric field controlled surface magnetic anisotropy and micromagnetic nucleation modes for $L1_0$-CoPt thin-film is investigated with density-functional and micromagnetic model calculations. The electric field redistributes electron states near the Fermi level, which has a fairly strong effect on the surface anisotropy, but due to inversion symmetry, the net anisotropy of the films with odd numbers of layers remains unchanged. By contrast, the micromagnetic nucleation mode is spatially asymmetric even for symmetric thin-films with odd numbers of layers. This leads to a reduction of the nucleation field (coercivity) and — for suitably chosen nanostructures — to substantial changes in the hysteretic behavior. In lowest order, the coercivity reduction is independent of the total film thickness. This counter-intuitive feature can potentially be exploited in magnetoelectric switching devices.

Index Terms—Magneto-electronics, thin-films.

I. INTRODUCTION

The effect of electric fields on the magnetic anisotropy has recently attracted much attention, with substantial anisotropy changes in some systems [Weisheit 2007, Niranjan 2010, Velev 2011]. The magnetoelectric effect is scientifically interesting and technologically important for applications such as electrically controlled magnetic data storage and switching devices for spin electronics [Velev 2011]. The phenomenon was initially observed in multiferroic materials, where ferromagnetism and ferroelectricity coexist in the same phase. The corresponding bulk magnetoelectric effect is due to the structural deformation induced by an electric field and limited to low temperatures [Eerenstein 2006, Ramesh 2007]. This limitation does not exist in ferromagnetic thin films and nanostructures, which have recently sparked much interest in the context of low-power spintronic devices. This was first demonstrated by showing that the coercivity of $L1_0$-FePd and FePt thin films can be modified by an applied electric field when the films are immersed in a liquid electrolyte [Weisheit 2007]. Electric-field induced modifications of intrinsic magnetic properties, such as anisotropy and magnetization, are now well established at ferromagnetic surfaces and interfaces; they have been observed experimentally [Maruyama 2009, Shiota 2009] and described theoretically [Tsujikawa 2009, Manchanda 2011, 2014]. At ferromagnetic surfaces and interfaces, an external electric field modifies the magnetic anisotropy through an electronic mechanism, via a spin-dependent screening of the electrons at the surface in which the electron screens the electric field over the screening length of the metal. The atomic origin of this anisotropy change is well understood [Duan 2008, Manchanda 2013, Ruiz-Díaz 2013].

Compared to the electric-field effects on intrinsic properties, the interplay between electric fields and static micromagnetism is an important but as yet uninvestigated question. Numerical methods to study the effect of electric fields on dynamical magnetic properties in magnetoelectric materials are being developed [Fischbacher 2011], and it has also been shown that dynamical effects such as domain-wall motion can be modified via electric control of intrinsic magnetic properties [Lahtinen 2012, van de Wiele 2014] and ferrite garnet films [Logginov 2007]. Recently, magnetization switching due to picosecond electric field pulses in MgO/FePt/Pt(001) films has been predicted using first-principle and micromagnetic simulations [Zhu 2014]. This switching occurs via uniform or Stoner-Wohlfarth magnetization reversal, which is usually the physically realized mechanism as the structural feature sizes of magnetic nanostructures become very small [Skomski 2003]. The control of spin wave frequencies through magnetoelectric pinning is calculated recently by Moore *et al* [2014]. The pinning of dynamic magnetization at the interface with interface Dzyaloshinskii-Moriya interaction is observed [Kostylev 2014].

In this Letter, we investigate the effect of an electric field on the magnetic anisotropy and coercivity of thin-films, using $L1_0$-ordered CoPt(001) as an example. We have chosen this material, because it has attracted much attention in other contexts [Coffey 1995, Jeong 2000, Zeng 2002] and exhibits large

Corresponding author: P. Manchanda (pmanchanda2@unl.edu).

perpendicular anisotropy. We use numerical methods, including VASP, and micromagnetic model calculations to determine both intrinsic and extrinsic properties of the films and show that nonuniform reversal effects persist as the total film thickness approaches atomic dimensions.

Fig. 1 shows the considered $L1_0$-CoPt thin films (a = 3.806 Å, c =3.684 Å [Villars 2000]), which contain odd and even numbers of monolayers and correspond to the stoichiometries Co_4Pt_3 and Co_3Pt_3, respectively. This system is chosen to ensure a perpendicular magnetic anisotropy. The films are located between but not connected to the electrodes, and there are

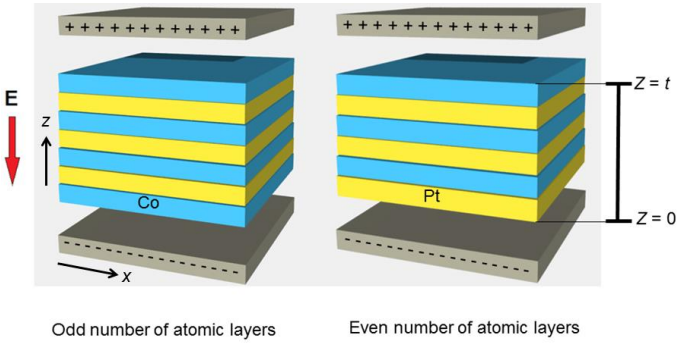

Fig.1. The $L1_0$-CoPt thin-film system considered in this paper.

no stationary currents in the system. The micromagnetic description of the films, that is, the determination of nucleation field H_N or coercivity $H_c \approx H_N$, requires the knowledge of the local anisotropy $K_1(\mathbf{r}) = K_1(z)$. Due to the screening by conduction electrons, the modification of $K_1(z)$ has the character of a magnetic surface anisotropy that depends on the electric field, with generally different values for the top and bottom surfaces. We start by first determining $K_1(z)$ from first principles.

II. COMPUTATIONAL DETAILS

The first-principle calculations were carried out in the framework of density functional theory (DFT), using the projected augmented wave (PAW) method as implemented in the Vienna *ab-initio* simulation package (VASP) [Kresse 1994]. The exchange and correlations are described by a spin-polarized generalized-gradient approximation using the Perdew-Burke-Ernzerhof (PBE) functional [Perdew 1996]. The energy cutoff for the plane-wave basis set was taken to be 450 eV, and we have used a 13 × 13 × 1 Monkhorst-Pack grid for the k-point sampling in the self-consistent calculations [Monkhorst 1976]. Structural relaxations were performed until the Hellmann-Feynman forces on the relaxed atoms become less than 0.01 eV/Å. The external electric field was introduced by the planar dipole layer method [Neugebauer 1992], where dipole centered in the vacuum region of the supercell. Fully relativistic self-consistent calculations including spin-orbit coupling have been carried out to determine the magnetocrystalline anisotropy energy (MAE) by taking the difference between the self-consistent total energy for the magnetization orientation perpendicular (001) and parallel (100) to the surface.

III. RESULTS

The electric field modifies the electron states and occupancies in the film, which is the reason for the anisotropy change. Due to screening, the redistribution predominantly affects the atoms near the surface. Fig.2 shows the *change* in spin density due to an electric field of 0.6 V/Å, projected onto the x-z and x-y plane. We see that the applied electric field changes the spin density of the surface Co and Pt atoms significantly, with much smaller changes in the middle of the film.

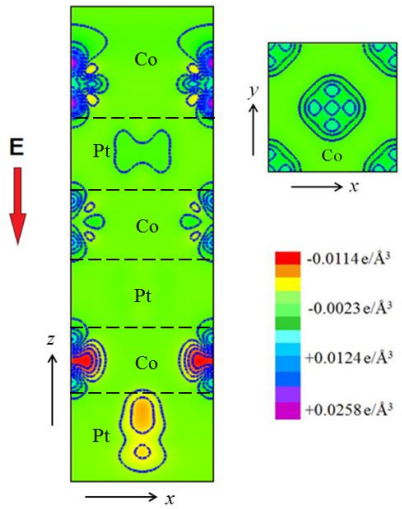

Fig. 2. Induced spin density change, $\Delta\sigma = \sigma(E) - \sigma(0)$, for Co_3Pt_3 in the presence of an electric field E = 0.6 V/Å, projected onto the x-z plane(left) and x-y plane (right). Where dashed lines indicates the nominal boundaries between Co and Pt.

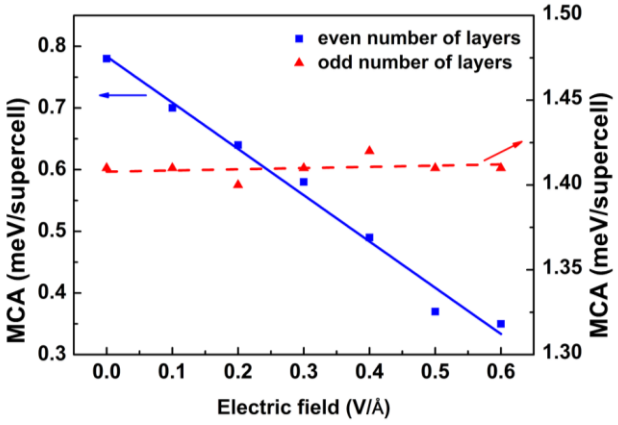

Fig. 3. Calculated magnetocrystalline anisotropy (MCA) energies for odd (dashed red line) and even (solid blue line) number of layers. These anisotropies (1meV ~ 10 MJ/m^3 = 10 Merg/cm^3) are sufficiently strong to overcome the shape anisotropy [Skomski 2003] and to ensure a preferred magnetization direction perpendicular to the film.

Fig. 3 shows the calculated magneto-crystalline anisotropy (MCA) energy per supercell as a function of electric field; the numbers of atoms per supercell are 14 and 12 for the Co_4Pt_3 and Co_3Pt_3, respectively. The anisotropy of the Co_3Pt_3 system decreases linearly with increasing electric field (solid-blue line in Fig. 3), whereas the anisotropy of the Co_4Pt_3 system remains unchanged as a function of the electric field. Due to the redistribution of electron states near the Fermi level, the application of a perpendicular electric field yields a fairly strong change in the surface anisotropy. However, for odd number of layers, the top and bottom contributions nearly completely cancel each other, so that the net change in the total anisotropy energy is zero (dashed red line in Fig. 3). There is also some anisotropy variation inside the films, but due to screening, this anisotropy is independent of electric field.

The nucleation modes have been determined via analytical model calculations using magnetic anisotropy obtained from first principles. Following the procedure outlined in Ref. Skomski 2003, the nucleation field is determined from the differential equation

$$-A\nabla^2\phi + K_1(\mathbf{r})\phi + \frac{1}{2}\mu_0 M_s H\phi = 0 \qquad (1)$$

Here $A \approx 10$ pJ/m is the exchange stiffness of CoPt alloys, M_s is the saturation magnetization, H is the external magnetic field and $\phi(\mathbf{r})$ is the nucleation mode, that is, the angle between magnetization and c-axis near the onset of magnetization reversal. nucleation is an eigenvalue problem. Note that the nucleation field is similar to the eigenfrequency of a mechanical harmonic oscillator, which is independent of the amplitude of the oscillation in lowest order.

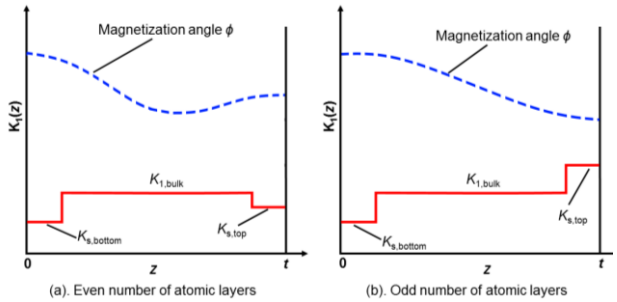

FIG. 4. Anisotropy profiles $K_1(z)$ (red) and nucleation modes $\phi(z)$ (blue) for (a) even and (b) odd numbers of atomic layers.

To solve (1), the surface anisotropy is modeled as a δ-function [Skomski 2007].

$$K_1(\mathbf{r}) = K_{1,bulk} + K_{s,bottom}\delta(z) + K_{s,top}\delta(z-t) \qquad (2)$$

where $K_{s,bottom}$ and $K_{s,top}$ depend on the termination of the bottom and top surfaces, respectively.

Fig. 4 shows how the anisotropy profiles translate into a nucleation mode. For odd numbers of layers, the net anisotropy change is zero. However, due to the electric-field-dependent surface anisotropy, one surface becomes somewhat softer (reduced K_1), whereas the opposite surface becomes harder by the same amount (enhanced K_1). Nucleation always starts in the softest region of the magnet, that is, near $z = 0$ in as shown in Fig. 4.

In other words, both the nucleation mode $\phi(z)$ and the nucleation field H_N are predominantly determined by the surface with reduced $K_1(z)$. For *even* numbers of atomic layers, Fig. 4(a), the net anisotropy change is nonzero, because the top and bottom surfaces are chemically different. The nucleation field increases or decreases in a straightforward manner, according to the Stoner-Wohlfarth anisotropy field $H_N = 2\langle K\rangle/\mu_o M_s$ and depending on the direction of the electric field.

For films with *odd* numbers of atomic layers, Fig. 4(b), the micromagnetic analysis is somewhat less straightforward. The lowest-order electric-field contribution to the nucleation field is $\phi(z) \sim \cos(\pi z/t)$, This mode is antisymmetric with respect to the film center and admixed to the Stoner-Wohlfarth mode $\phi = const$. The resulting mode, shown in Fig. 4(a), is therefore neither symmetric nor antisymmetric. Using (1) and diagonalizing the corresponding 2 × 2 mode-coupling matrix yield the nucleation field.

$$H_N = \frac{2}{\mu_0 M_s}\left(K_1 - \frac{2K_s^2}{\pi^2 A}\right) \qquad (3)$$

where $K_s(E)$ is the surface-anisotropy change at the top or bottom of the film.

A striking feature of (3) is that this nucleation field is independent of film thickness. Normally, surface anisotropy corresponds to an effective bulk anisotropy correction $\Delta K = K_s/t$ [Gradmann 1993], so that the relative surface effect should decrease with increasing film thickness. However, the nucleation mode in Fig. 4 is nonuniform and therefore costs exchange energy, $\int A\,(\partial\phi/\partial z)^2\,dz \sim A/t$. A physical explanation is that the surface anisotropy becomes less effective with increasing film thickness, but the nucleation mode costs less exchange energy, and the two effects cancel each other. The outcome of this competition is a film-thickness-independent nanoscale magnetoelectric surface correction to the nucleation field, in spite of the atomic origin of the underlying surface anisotropy of (2). Note also that (3) is independent of the sign of K_s, which is a consequence of the inversion symmetry of Co_4Pt_3.

It is instructive to look at the film-thickness dependence of the nucleation field from the opposite limit of thick films. In this limit, the two surfaces are well-separated and the corresponding lowest-lying micromagnetic modes, as predicted by (1-2), do not talk to each other. This means that nucleation field is entirely determined by the anisotropy minimum of Fig. 4(b). As the film gets thinner, the two surfaces become connected micromagnetically — not electronically! — and from Fig. 4(b), one intuitively expects that this interaction leads to a complete micromagnetic averaging in the ultrathin-film limit. However,

(3) show that is this is not the case.

IV. CONCLUSIONS

In summary, we have shown that even in inversion-symmetric thin-films, where the net anisotropy remains *unchanged*, an electric field creates a nonzero micromagnetic response. The effect is independent of the total film thickness, because the thickness-dependent net anisotropy and exchange-energy contributions cancel each other. The underlying micromagnetic parameters can be determined from first principles, using VASP supercell calculations for different mulilayer terminations. The results of this paper are expected to lead to future experimental and computational research on micromagnetic aspects of magnetoelectric materials.

ACKNOWLEDGEMENT

This research is supported by ARO (W911NF-10-2-0099) and NSF MRSEC (DMR-0820521). Computations were performed at the University of Nebraska Holland Computing Center.

REFERENCES

Coffey K R, Parker M A, and Kent Howard J (1995), "High anisotropy $L1_0$ thin films for longitudinal recording," IEEE Trans. Magn. vol. 31, pp. 2737-2739.

Duan C G, Velev J P, Sabirianov R F, Zhu Z, Chu J, Jaswal S S, and Tsymbal E Y (2008), "Surface magnetoelectric effect in ferromagnetic metal films," Phys. Rev. Lett., vol. 101, pp. 137201.

Eerenstein W, Mathur N D, and Scott J F (2006), "Multiferroic and magnetoelectric materials,"Nature, vol. 442, pp. 759-765.

Fischbacher T, Franchin M, and Fangohr H, "Micromagnetic simulations of magnetoelectric materials (2011)," J. Appl. Phys. vol. 109, pp. 07D352.

Gradmann U, Handbook of Magnetic materials, Vol. 7, Ed.: Buschow K H J, Elsevier, Amsterdam (1993).

Jeong S, Hsu Y –N, Laughlin D E, and McHenry M E (2000), "Magnetic properties of nanostructured CoPt ad FePt thin films" IEEE Trans. Magn. vol. 36, pp. 2336-2338.

Kostylev M (2014), "Interface boundary conditions for dynamic magnetization and spin wave dynamics in a ferromagnetic layer with the interface Dzyaloshinskii-Moriya interaction" J. Appl. Phys., vol. 115, pp. 233902.

Kresse G and Joubert D (1999), "From ultrasoft pseudopotential to the projector augmented-wave method," Phys. Rev. B vol. 59, 1758-1775.

Logginov A S, Meshkov G A, Nikolaev A V, and Pyatakov A P (2007), "Magnetoelectric control of domain walls in a ferrite garnet film,"JETP Lett. vol. 86, pp. 115-118.

Lahtinen T H E, Franke K J A, van Dijken S (2012), "Electric-field control of magnetic domain wall motion and local magnetization," Sci. Rep. vol. 2, pp. 258.

Manchanda P, Skomski R, Solanki A K, Kumar P S A, Kashyap A. (2011), "Magnetoelectric effect in $L1_0$-CoPd thin films," IEEE Trans. Magn. vol. 47, pp. 4391.

Manchanda P, Kumar P, Skomski R, and Kashyap A (2013), "Magnetoelectric effect in organometallic vanadium-benzene wires," Chem. Phys. Lett. vol. 568, pp. 121-124.

Manchanda P, Skomski R, Prabhakar A, and Kashyap A. (2014), "Magnetoelectric effect in Fe linear chains on Pt(001), "J. Appl. Phys. vol. 115, pp. 17C733.

Maruyama T, Shiota Y, Nozaki T, Ohta K, Toda N, Mizuguchi M, Tulapurkar A A, Shinjo T, Shiraishi M, Mizukami S, Ando Y, and Suzuki Y (2009), "Large voltage-induced magnetic anisotropy change in a few atomic layers of iron," Nat. Nanotech. vol. 4, pp. 158-161.

Monkhorst H J and Pack J D (1976), "Special points for Brillouin-zone integrations, " Phys. Rev. B vol. 13, pp. 5188-5192.

Moore T, Camley R E, K L Livesey (2014), "Spin waves in a thin film with magnetoelectric coupling at the surfaces," J. Magn. Magn. Mater. vol. 372, pp. 107-111.

Neugebauer J and Scheffler M (1992), "Adsorbate-substrate and assorbate-adsorbate interactions of Na and K adlayers on Al(111) (1992)," Phys. Rev. B vol. 46, 16067-16080.

Niranjan M K, Duan C G, Jaswal S S, and Tsymbal E Y (2010), "Electric field effect on magnetization at the Fe/MgO(001) interface,"Appl. Phys. Lett. vol. 96, pp. 222504.

Perdew J P, Burke K, and Ernzerhof M (1996), "Generalized gradient approximation made simple," Phys. Rev. Lett. vol. 77, pp. 3865-3868.

Ramesh R, and Spaldin N A (2007), "Multiferroics: progess and prospects in thin films," Nature Mater., vol. 6, pp. 21-29.

Ruiz-Díaz P, Dasa T R, and Stepanyuk V S (2013), "Tuning magnetic anisotropy in metallic multilayers by surface charging: An *ab-initio* study," Phys. Rev. Lett., vol. 110, pp. 267203.

Shiota Y, Maruyama T, Nozaki T, Shinjyo T, Shiraishi M, and Suzuki Y (2009), "voltage-assisted magnetization switching in ultrathin $Fe_{80}Co_{20}$ alloy layers," Appl. Phys. Express, vol. 2, pp. 063001.

Skomski R (2003), "Nanomagnetics," J. Phys.: Condens. Matter vol. 15, pp. R841-R896R.

Skomski R, Wei X H, and Sellmyer D J (2007), "Magnetization reversal in cubic nanoparticles with uniaxial surface anisotropy," IEEE Trans. Magn. vol. 43 (6), pp. 2890-2892.

Tsujikawa M and Oda T (2009), "Finite electric field in the large perpendicular magnetic anisotropy surface Pt/Fe/Pt(001): A first-principle study," Phys. Rev. Lett. vol. 102, pp. 247203.

Weisheit M, Fähler S, Marty A, Souche Y, Poinsignon C, Givord D (2007), "Electric field-induced modification of magnetism in thin-film ferromagnets," Science, vol. 315, pp. 349-351.

Velev J P, Jaswal S S, and Tsymbal E Y (2011), "Multiferroic and magnetoelectric materials and interfaces," Phil. Trans. R. Soc. A, vol. 369, pp. 3069-3097.

van de Wiele B, Laurson L, Franke K J A, and van Dijken S (2014), "Electric field driven magnetic domain wall motion in ferromagnetic-ferroelectric heterostructures" Appl. Phys. Lett. vol. 104, pp. 012401.

Villars P, and Calvert L D, Pearson's Handbook of Crystallographic Data for Intermetallic Phase (Meta Park, OH, ASM, 2000).

Zeng H, Yan M L, Powers N, and Sellmyer D J (2002), "Orientation-controlled nonepitaxial $L1_0$ CoPt and FePt films, " Appl. Phys. Lett. vol. 80, pp. 2350.

Zhu W J, Xiao D, Liu Y, Gong S J, and Duan C G (2014), "Picosecond electric field pulse induced coherent magnetic switching in MgO/FePt/Pt(001)-based tunnel junctions: a multiscale study," Sci. Rep. vol. 4, pp. 4117.